Arab J. Nucl. Sci. Appl., Vol. 58, 3, 28-38 (2025)

ISSN 1110-0451

Arab Journal of Nuclear Sciences and Applications

Web site: ajnsa.journals.ekb.eg

(E S N S A)

Radiological Assessment of Handcrafted Pottery from some Regions in Upper Egypt

M. El-Zohry[1], Shaimaa T. Tawfik[2] and M. H. El-Zayat[3]*

[1] *Physics Department, Faculty of Science, Sohag University, Sohag, Egypt.*

[2]*Radiation Protection Department, Nuclear and Radiological Safety Research Center, Egyptian Atomic Energy Authority, Cairo, Egypt.*

[3]*Ph.D. of physic, QenaSTEM School, Ministry of Education, Egypt.*

ARTICLE INFO

Article history:

Received: 17th Mar. 2025

Accepted: 29th May 2025

Available online: 23rd June 2025

Keywords:

Radioactivity;
Radioactive analysis;
Radiation Hazard;
Marl clay;
Nile silt;
Handcrafted pottery.

ABSTRACT

A high-resolution HPGe (High Purity Germanium) detector, integrated with a low background γ-ray counting system, was used to perform a radioactive analysis of marl clay, Nile silt and pottery samples from handcrafted pottery production sites in Hijaza, Qena, Upper Egypt. The analysis focused on the activity concentrations of natural radionuclides namely ^{238}U, ^{232}Th and ^{40}K which are key contributors to environmental radioactivity. The average activity concentrations measured for ^{238}U, ^{232}Th and ^{40}K were found to be 13.72 ± 0.77 Bq/kg, 8.97 ± 0.39 Bq/kg and 94.91 ± 4.73 Bq/kg, respectively. Based on these activity concentrations, several radiation hazard indices were calculated, including radium equivalent activities, absorbed dose rates (D_{out}), the Gamma radiation representative level index (I_γ), Furthermore, the study estimated annual effective dose equivalent (D_{eff}), external and internal hazard indices (H_{ext} & H_{int}), excess lifetime cancer risk (ELCR) and the annual gonadal equivalent dose (AGED). These values were compared with globally recommended standards to assess the potential radiation hazard posed by the samples.

1. INTRODUCTION

Spanning a remarkable duration of over seven millennia, Egyptian potters have consistently fabricated a heterogeneous assortment of ceramic containers, employing fundamental resources and techniques that have, to a considerable degree, demonstrated notable continuity throughout this extensive historical trajectory [1, 2 and 3]. Marl clays and Nile silt have been the primary materials used in pottery production in Egypt throughout history [4 and 5]. Clay is a natural substance primarily composed of fine-grained minerals that exhibit plasticity when moistened and harden upon drying or firing. These minerals, typically silicates smaller than 2 microns, are abundant on the Earth's surface and can form shales and other sedimentary rocks [6]. In Egypt, marl and Nile alluvium are the most commonly used clays for pottery making. Marl is a calcareous clay derived from limestone and contains calcium carbonate, while Nile clay, also called Nile alluvium or Nile silt, is an organic-rich mud carried by the Nile River, which contains significant amounts of silica [7]. These materials naturally harbor radioactivity due to the decay of Uranium (^{238}U), Thorium (^{232}Th), and Potassium (^{40}K) isotopes [8, 9 and 10]. Given their origin, marl clay and Nile silt contain varying levels of natural radionuclides, which could pose a radiation risk. This risk stems from the potential radiation exposure to workers handling these naturally occurring radioactive materials, depending on the source of the raw material and the concentration of radionuclides present [10 and 11].

This research examined the potential radiation dangers linked to making and using pottery in the Hijaza region of Upper Egypt. The goal was to see if the raw materials or the finished products posed any radiological risks. The study is divided into four parts: first, how samples were collected and prepared; second, the equipment and methods used to detect radiation and assess its levels; third, an analysis of the findings; and finally, a summary and interpretation of what the results mean.

Corresponding author: mah.elzayat.1976@gmail.com

DOI: 10.21608/ajnsa.2025.369148.1881

Map (1): The location of the concerned sites

2. SAMPLES PREPARATION

A total of 15 representative samples of marl clay, Nile silt and pottery were collected from handcrafted pottery sites located in Hijaza, Qus, Qena, Upper Egypt. The samples procured were placed in plastic pouches and methodically marked. Marl clay and Nile silt samples were dried to remove the moisture content. The dried samples of marl clay, Nile silt and pottery samples were crushed into tiny particles using a grinder and screened through a 1 mm mesh sieve to ensure uniformity [12, 13 and 14]. The meshed samples were weighed and kept tightly closed in plastic containers of 100 cc made from polyethylene and left for a minimum of 30 days to attain a radioactive equilibrium to be reached [15 and 16]. The initial net weight of the sample was determined before undertaking the γ-ray spectrometric measurements.

3. GAMMA SPECTROMETRIC ANALYSIS

A gamma spectrometric analysis was carried out to examine the spectral properties of the samples. The study took place at the Radiation Protection Department of the Nuclear and Radiological Safety Research Center, Atomic Energy Authority, Egypt, utilizing an N-type HPGe coaxial detector. This detector featured a 40% relative efficiency and an energy resolution of 2.0 keV for 1.33 MeV photons emitted by ^{60}Co. To uphold quality assurance, reference materials with established levels of natural radioactivity were used. The Lab SOCS software was employed for mathematical efficiency calibration, ensuring accurate detector calibration for laboratory samples of identical geometric configurations. Spectral data underwent quantitative analysis with the CANBERRA (Genie 2000) software. Additionally, background measurements were conducted under identical conditions to those of the sample analysis, facilitating the correction of net peak areas of γ-rays from identified isotopes.

4. SAMPLES ANALYSIS AND ACTIVITY CONCENTRATIONS

Under secular equilibrium conditions, the activity concentration of ^{238}U was determined based on the gamma emission peaks of ^{214}Bi (609.3, 1120.3, and 1764 keV) and ^{214}Pb (351 keV). Similarly, the activity of ^{232}Th was calculated using the gamma peaks of ^{208}Tl (583.19 and 2614.53 keV), ^{212}Pb (238.63 and 300.09 keV), ^{228}Ac (911 keV) and ^{212}Bi (727.3 keV). The activity concentration of ^{40}K was directly obtained from its characteristic gamma peak at 1460.83 keV [17,18 and 19]. The activity concentrations of these natural radionuclides (^{238}U, ^{232}Th and ^{40}K) in the analyzed samples were calculated using the formula presented in Equation (1) [20, 21 and 22].

$$A_S = \frac{N_C}{M \times \varepsilon \times \phi} \ (Bq/kg) \qquad \textbf{(1)}$$

Where N_C is the net counting of γ-ray, M is the mass of the sample, ε is the detector efficiency and ϕ is the transition probability of γ-decay.

The elemental concentration of the radionuclide ^{238}U and ^{232}Th in (ppm) and ^{40}K in (%) in the measured samples were calculated from the activity concentrations in Bq/kg by using a specific conversion factor which is [22, 23, 24 and 25]: ^{238}U (ppm) = 12.35 Bq/kg of ^{238}U, ^{232}Th (ppm) = 4.06 Bq/kg of ^{232}Th and ^{40}K (%) = 313 Bq/kg of ^{40}K.

5. Radiological hazard indices

5.1. Radium equivalent (Ra_{eq})

The significant activity concentration of a sample, which contains varying levels of ^{238}U, ^{232}Th, and ^{40}K, accounts for both the external gamma radiation dose and the internal dose from radon and its decay products. This is summarized in a single radiological index known as the radium equivalent (Ra_{eq}), which is mathematically defined, as [26 and 27]:

$$Ra_{eq}\,(Bq/kg) = A_U + 1.43\,A_{Th} + 0.077\,A_K \quad \textbf{(2)}$$

Where $A_{(Ra)}$, $A_{(Th)}$ and $A_{(K)}$ stand for the activity of corresponding radionuclides ^{238}U, ^{232}Th and ^{40}K in Bq/kg respectively.

5.2. Absorbed dose rates (D_{out})

The external outdoor risk of exposure to terrestrial γ-rays in the air, at a height of 1 meter above the ground, was calculated based on the uniform distribution of naturally occurring radionuclides ^{238}U, ^{232}Th, and ^{40}K in trace amounts in the soil. It was assumed that other radionuclides, such as ^{137}Cs, ^{90}Sr and the ^{235}U decay series, contribute insignificantly to the total environmental radiation dose and were therefore excluded from the calculation. The calculation was carried out as follows:

$$D_{out}\,(nGyh^{-1}) = 0.462\,A_U + 0.621A_{Th} + 0.0417A_K \quad \textbf{(3)}$$

Where the coefficients of 0.462, 0.621 and 0.0417 are conversion factors in ($nGyh^{-1}$) per unit activity (Bq/kg) for dry weight of ^{238}U, ^{232}Th and ^{40}K [28 and 29].

5.3. Gamma representative index (I_γ)

Gamma representative Index (Iγ) is used to assess the level of gamma radiation hazard from natural gamma emitters. This index helps correlate the annual dose rate resulting from exposure to gamma radiation. To ensure that the radiation hazard remains minimal, Gamma representative Index (Iγ) should be less than unity. The Iγ index was calculated using the following equation [30 and 31]:

$$I_\gamma = A_U/150 + A_{Th}/100 + A_K/1500 \quad \textbf{(4)}$$

5.4. Alpha index (I_α)

The internal Alpha index addresses the increased level of alpha radiation resulting from radon inhalation. It was calculated using the following equation [32 and 33]:

$$I_\alpha = A_U\,/200\ (Bq/kg) \quad \textbf{(5)}$$

Where A_U is the specific activity of ^{226}Ra. The maximum value of the alpha index is unity.

5.5. Annual effective dose equivalent (D_{eff})

The annual effective dose equivalent ($mSvyr^{-1}$) is calculated from the absorbed dose rate by applying a dose conversion factor of 0.7 Sv/Gy for an adult, as reported by UNSCEAR 2008, along with an occupancy factor of 0.4 for the time spent working with pottery. The effective dose (D_{eff}) Is quantified through the following equations [34, 35 and 36]:

$D_{eff}\ (mSvyr^{-1}) = D\ (nGyh^{-1}) \times 8760\ h \times 0.7 \times (103\ mSv/109\ nGy) \times 0.2,$

$$D_{eff}\,(mSvyr^{-1}) = D\,(nGyh^{-1}) \times 1.21 \times 10{-}3\ (mSvyr^{-1}) \quad \textbf{(6)}$$

The global annual effective dose equivalent (D_{eff}) from natural radiation sources in areas with normal background radiation is estimated to be 1 $mSvyr^{-1}$, according to UNSCEAR 2000.

5.6. External and Internal Indices (H_{ext} & H_{int})

To evaluate the external radiological hazard from exposure to γ-radiation, a widely used criterion is the external hazard index (H_{ext}). It is calculated as follows [37 and 38]:

$$H_{ext} = A_U\,/370 + A_{Th}/259 + A_K/4810 \quad \textbf{(7)}$$

In addition to the external hazard, radon and its short-lived decay products pose a risk to the respiratory system. Internal exposure to radon and its daughters is quantified using the internal hazard index (H_{int}), which is calculated using the following equation [37 and 38]:

$$H_{int} = A_U\,/185 + A_{Th}\,/259 + A_K\,/4810 \quad \textbf{(8)}$$

The values of H_{ext} and H_{int} must be below unity in order to ensure that the radiation hazard remains insignificant.

5.7. Excess lifetime cancer risk (ELCR)

The potential risk of developing or being diagnosed with cancer due to outdoor exposure, assuming a lifetime average daily exposure over 70 years, was computed using the following equation [39]:

$$ELCR = D_{eff}\,(mSvyr^{-1}) \times D_L \times R_F \quad \textbf{(9)}$$

In this equation, D_{eff} denotes the annual effective dose equivalent, D_L refers to the lifespan duration (70 years) and R_F represents the cancer risk factor, accounting for stochastic effects. The R_F value is 0.05/Sv for the general public.

5.8. Annual gonadal equivalent dose (AGED)

The annual gonadal dose equivalent resulting from the activity concentrations of ^{226}Ra, ^{232}Th and ^{40}K is mathematically formulated as follows. [40]:

$$AGED\ (mSvyr^{-1}) = 3.09A_U + 4.18A_{Th} + 0.314\ A_K \quad \textbf{(10)}$$

The organs of interest by UNSCEAR include the thyroid, lungs, bone marrow, bone surface cells, gonads and the female breast.

6. RESULTS AND DISCUSSIONS

The activity concentrations of natural radionuclides ^{238}U, ^{232}Th and ^{40}K in the analyzed samples, along with the corresponding Th/U, K/U and K/Th ratios, are presented in Table 1. As depicted in Table 1 and Figure 1, the measured activity concentrations across all sample types ranged from 1.42 ± 0.118 Bq/kg to 27.10 ± 0.43 Bq/kg for ^{238}U, with an average value of 13.72 ± 0.77 Bq/kg. The concentration of ^{232}Th varied between 8.97 ± 0.39 Bq/kg and 94.91 ± 4.73 Bq/kg, with an average value of 94.91 ± 4.73 Bq/kg, while ^{40}K levels ranged from 34.01 ± 2.01 Bq/kg to 175.86 ± 2.87 Bq/kg. Among the three radionuclides, ^{40}K exhibited the highest specific activity, followed by ^{238}U and ^{232}Th.

For all analyzed samples, the specific activity concentrations of ^{238}U, ^{232}Th and ^{40}K remained below the internationally recognized safety limits established by UNSCEAR (2000), which are 35 Bq/kg for ^{238}U, 30 Bq/kg for ^{232}Th and 400 Bq/kg for ^{40}K.

The elemental ratio for ^{232}Th ranged from 0.37 ppm to 6.67 ppm, with an average of 2.21 ppm. Similarly, ^{238}U varied between 0.85 ppm and 2.11 ppm, with an average of 1.11 ppm. The potassium concentration (K%) for ^{40}K spanned from 0.11% to 0.56%, averaging 0.30%.

Table 1, along with Figures 3, 4 and 5, illustrates a noticeable correlation between the pairs ^{232}Th and ^{238}U, ^{40}K and ^{238}U and ^{232}Th and ^{40}K. As shown in Table 1 and Figures 3, 4 and 5, the Th/U ratio varied between 0.125 and 1.255, with an average value of 0.653 and a linear regression coefficient of 45%. The K/U ratio ranged from 1.327 to 14.755, with an average of 6.916, which is lower than the global average of 11.43 [41] and exhibited a very weak correlation of 0.1%. The K/Th ratio varied from 2.272 to 24.37, with an average of 13.91, which surpasses the global average of 13.33 [41] and demonstrated a linear regression coefficient of 52%.

The calculated radium equivalent (Ra_{eq}) values in Bq/kg for the present study are presented in Table 2. As shown in Table 2 and Figure 2, the Ra_{eq} values ranged from 15.35 Bq/kg to 73.67 Bq/kg, with an average of 33.85 Bq/kg, which remains well below the recommended maximum value of 370 Bq/kg [42].

Table (1): The activity concentrations in (Bq/kg), (ppm) units, K%, Th/U, K/U and K/Th of ^{238}U, ^{232}Th and ^{40}K of the marl clay, Nile silt and pottery samples.

Sample Code	Activity concentration (Bq/kg)			^{238}U (ppm)	^{232}Th (ppm)	^{40}K%	Th/U	K/U	K/Th
	^{238}U	^{232}Th	^{40}K						
M1	10.47±0.39	1.52±0.12	35.21±2.07	0.848	0.373	0.112	0.145	3.361	23.224
M2	12.86±0.44	1.62±0.12	34.01±2.01	1.041	0.395	0.109	0.125	2.651	21.262
M3	10.94±0.43	1.42±0.118	36.2182±2.18	0.885	0.367	0.116	0.136	3.316	24.366
M4	12.46±0.50	1.64±0.14	35.44±2.33	1.009	0.413	0.113	0.134	2.845	21.160
M5	12.48±0.44	5.27±0.37	36.12±2.21	1 .010	1.280	0.115	0.416	2.895	6.952
P1	11.36±0.39	8.02±0.32	101.54±4.83	0.920	1.991	0.324	0.711	8.936	12.560
P2	13.25±0.41	8.32±0.42	104.96±2.97	1.073	2.058	0.334	0.631	7.895	12.518
P3	10.97±0.63	8.24±0.34	107.00±2.01	0.888	2.030	0.342	0.751	9.762	12.993
P4	11.94±0.40	8.62±0.42	108.15±2.16	0.967	2.121	0.348	0.721	9.113	12.641
P5	13.23±0.43	8.03±0.43	108.14±2.15	1.072	1.979	0.347	0.607	8.201	13.510
C1	11.22±0.39	13.77±0.44	165.43±2.43	0.908	3.391	0.529	1.227	14.755	12.022
C2	21.60±3.43	27.10±0.43	173.11±10.14	1.749	6.675	0.553	1.255	8.009	6.384
C3	14.08±0.45	13.40±0.47	175.86±2.87	1.140	3.301	0.560	0.952	12.439	13.067
C4	26.00±2.35	15.18±1.27	34.51±2.06	2.105	3.739	0.110	0.584	1.327	2.272
C5	13.00±0.41	12.23±0.43	167.74±7.53	1.053	3.013	0.536	0.941	12.904	13.712
Average	13.72±0.77	8.97±0.39	94.91±4.73	1.111	2.208	0.303	0.653	6.916	13.910
Min	10.47±0.39	1.42±0.118	34.01±2.01	0.848	0.367	0.109	0.125	1.327	2.272
Max	26.00±3.43	27.10±0.43	175.86±2.87	2.105	6.675	0.560	1.255	14.755	24.366

To reduce the hazardous impact of radon and its progeny on respiratory organs, both the internal (H_{in}) and external (H_{ex}) hazard indices must remain below 1 [41]. The results for the H_{in} and H_{ex} indices are summarized in Table 2 and illustrated in Figure 6. The H_{in} values range from 0.07 to 0.26, with an average of 0.13, while H_{ex} values vary between 0.03 and 0.17, averaging 0.07. All measured values remain well below the recommended upper limit of 1 [41].

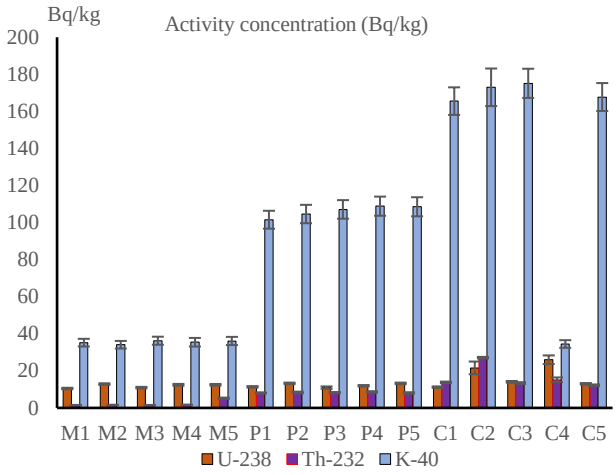

Fig. (1): The activity concentrations in (Bq/kg) of ^{238}U, ^{232}Th and ^{40}K of the marl clay, Nile silt and pottery samples.

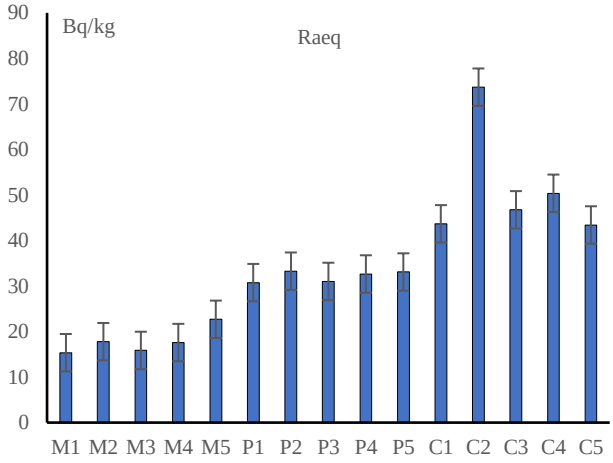

Fig. (2): The radium equivalent in (Bq/kg) of ^{238}U, ^{232}Th and ^{40}K for the marl clay, Nile silt and pottery samples.

Table (2): The radiological hazard indices of Ra_{eq}, H_{in}, H_{ex}, D_{out}, D_{eff}, ELCR, AGED I_γ and I_α for all measured samples

Sample Code	Ra_{eq} (Bq/kg)	H_{ex}	H_{in}	D_{out} (nGyh^{-1})	D_{eff} (mSvyr^{-1})	ELCR $\times 10^{-3}$	AGED (μSvyr^{-1})	I_γ (Bq/kg)	I_α (Bq/kg)
M_1	15.35	0.035	0.070	7.22	0.009	0.031	49.76	0.108	0.052
M_2	17.77	0.042	0.083	8.33	0.010	0.036	57.13	0.124	0.064
M_3	15.86	0.036	0.072	7.46	0.009	0.032	51.40	0.112	0.055
M_4	17.58	0.041	0.081	8.25	0.010	0.035	56.63	0.123	0.062
M_5	22.69	0.055	0.095	10.41	0.013	0.045	71.62	0.159	0.062
P_1	30.74	0.064	0.114	14.37	0.018	0.062	100.79	0.224	0.057
P_2	33.26	0.070	0.126	15.53	0.019	0.067	108.73	0.242	0.066
P_3	31.01	0.064	0.113	14.51	0.018	0.062	101.99	0.227	0.055
P_4	32.64	0.068	0.120	15.26	0.019	0.066	107.08	0.238	0.060
P_5	33.08	0.069	0.125	15.49	0.019	0.067	108.55	0.241	0.066
C_1	43.66	0.087	0.148	20.40	0.025	0.088	144.20	0.323	0.056
C_2	73.67	0.167	0.257	33.56	0.041	0.14	234.34	0.530	0.108
C_3	46.73	0.093	0.164	21.90	0.027	0.09	154.53	0.345	0.070
C_4	50.37	0.130	0.206	22.62	0.028	0.097	154.63	0.348	0.130
C_5	43.41	0.086	0.152	20.39	0.025	0.088	143.97	0.321	0.065
Min.	15.35	0.03	0.07	7.22	0.01	0.03	49.76	0.11	0.069
Max.	73.67	0.17	0.26	33.56	0.04	0.14	234.34	0.53	0.052
Average	33.85	0.07	0.13	15.71	0.02	0.07	109.69	0.244	0.130

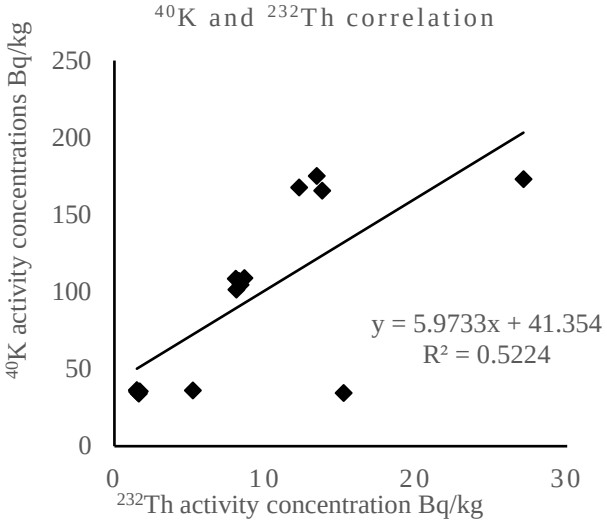

Fig. (3): Correlation between ^{238}U and ^{232}Th for all measured samples.

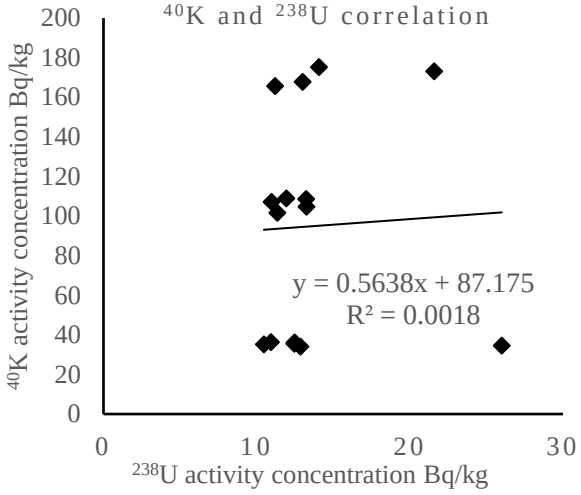

Fig. (4): Correlation between ^{238}U and ^{40}K for all measured samples.

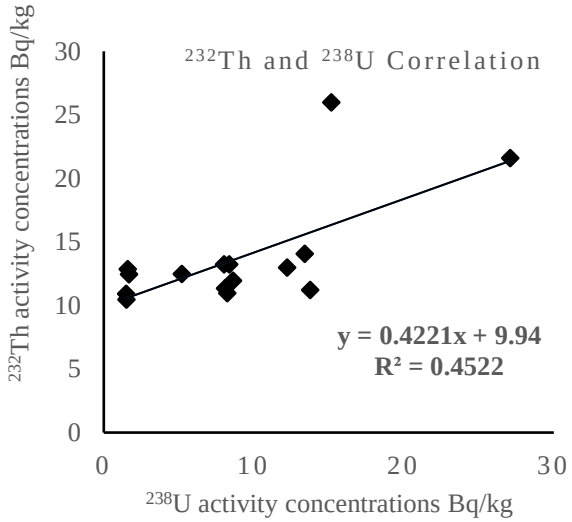

Fig. (5): Correlation between ^{40}K and ^{232}Th for all measured samples.

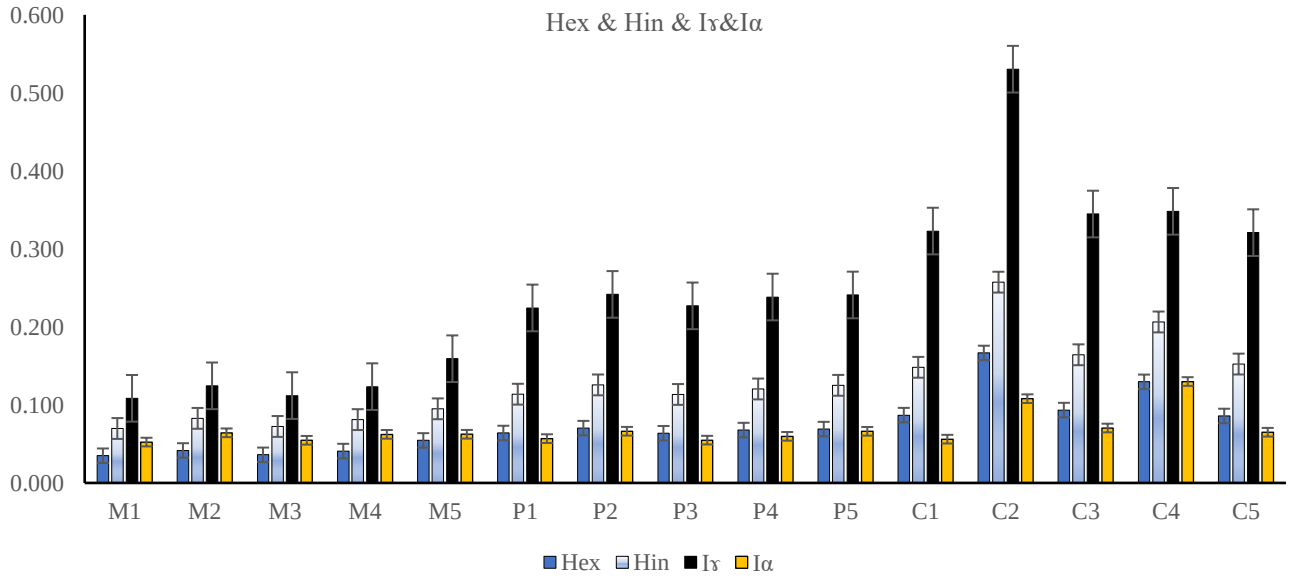

Fig. (6): The radiological hazard indices of H_{in} & H_{ex} & I_γ & I_α for all measured samples.

The results for the gamma index (Iγ) and the alpha index (Iα) are summarized in Table 2 and Figure 7. The values for the gamma index (Iγ) in all the measured samples ranged from 0.11 to 0.53 Bq/kg, with an average of 0.24 Bq/kg, which is below the permissible limit of 1 Bq/kg [41]. The alpha index (Iα) ranged from 0.052 to 0.069 Bq/kg, with an average of 0.130 Bq/kg, which is less than unity, indicating that the studied samples have a radium content significantly lower than the recommended upper limit of 200 Bq/kg [41].

The calculated values of the outdoor absorbed dose rate due to γ-ray exposure are shown in Table 2 and Figure 7. The results indicate that the absorbed dose rate ranged from 7.22 to 33.56 nGy/h, with an average of 15.71 nGy/h. Overall, the calculated outdoor absorbed dose rates for all the measured sample types are below the global average limit of 57 nGy/h, as reported by UNSCEAR 2000.

Table 2 and Figure 8 present a summary of the calculated values of the annual effective dose equivalent for the study samples. According to the results in Table 2, the annual effective dose equivalent values ranged from 0.01 mSv/year to 0.04 mSvyr^{-1}, with an average value of 0.02 mSvyr^{-1}. All the D_{eff} values (in mSv/year) for the study samples are below the ICRP recommended limit of 1 mSvyr^{-1} [43].

Based on the computed values of the annual effective dose, the excess lifetime cancer risk (ELCR) was evaluated using Equation 10 and is presented in Table 2 and Figure 9. The ELCR values ranged from 0.03 × 10^{-3} to 0.14 × 10^{-3}, with an average of 0.07 × 10^{-3}. All recorded ELCR values remain below the globally recommended limit of 0.29 × 10^{-3} [41].

The calculated values of the annual gonadal dose equivalent (AGDE) for the studied samples are provided in Table 2 and Figure 10. According to the results in Table 2, the AGDE values ranged from 49.76 μSvyr^{-1} to 234.34 μSvyr^{-1}, with an average value of 109.69 μSvyr^{-1}. For all samples, the AGDE values are below the global average value of 298 μSvyr^{-1} [41].

Figures 11, 12 and 13 show the results of the X-ray diffraction (XRD) analysis conducted using a Brucker (Asx-D&Advance) powder diffractometer at room temperature with Cu(Ka) radiation (λ = 1.5406 Å) under ambient conditions. The analysis of the investigated samples revealed the presence of potassium in the clay, marl clay and pottery samples, with distinct diffraction peaks corresponding to its essential components at various orientations.

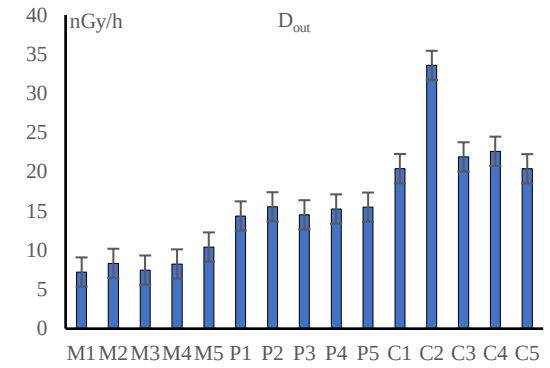

Fig. (7): The outdoor absorbed dose rate in (nGy/h) for all measured samples

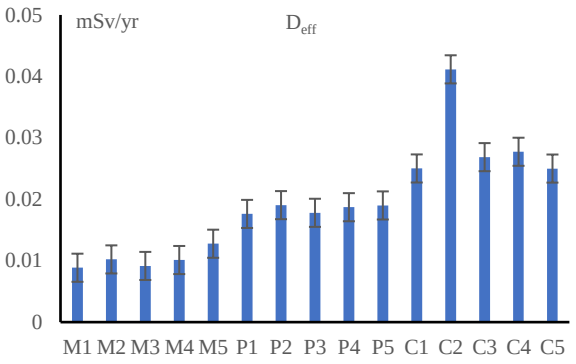

Fig. (8): The annual effective dose equivalent in (mSv/h) for the measured samples

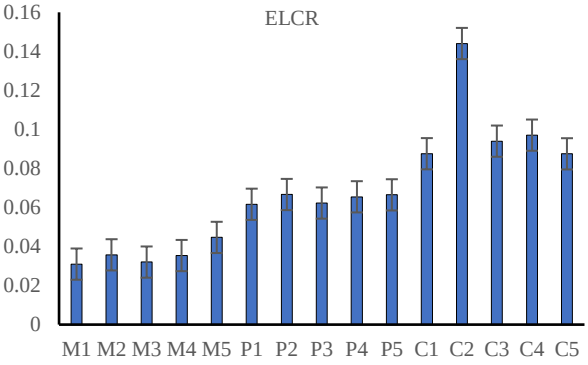

Fig. (9): The excess lifetime cancer risk for all measured samples.

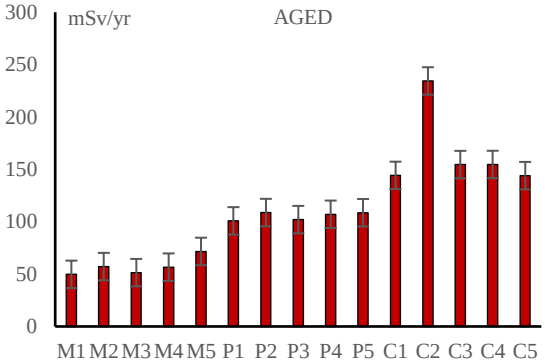

Fig. (10): The annual gonadal dose equivalent in μSvyr-1 for all measured samples.

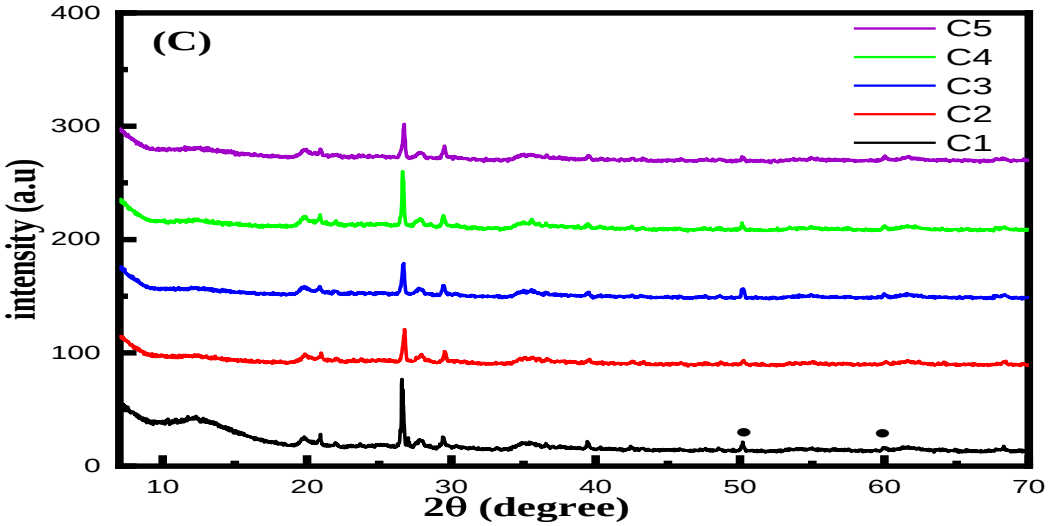

Fig. (11): The XRD for Nile silt samples

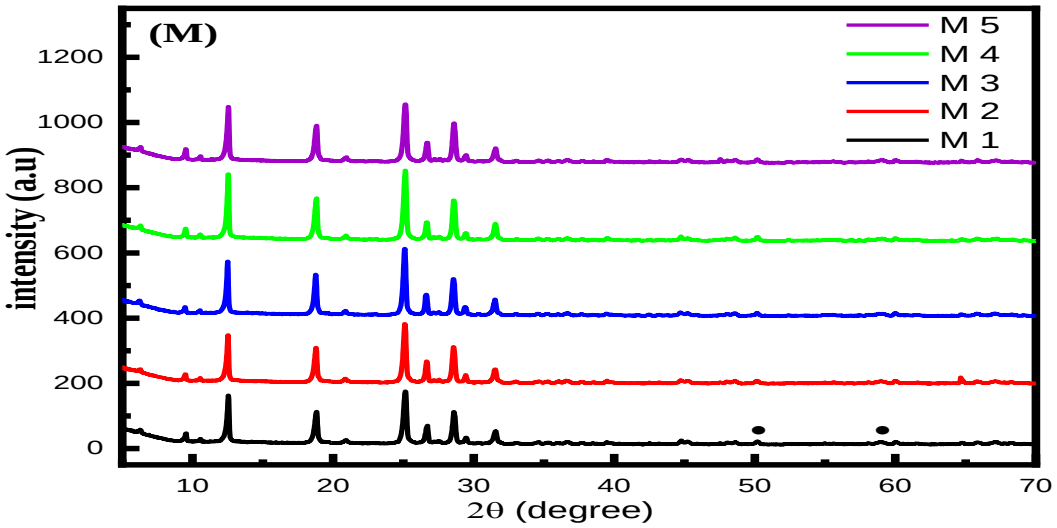

Fig. (12): The XRD for marl clay

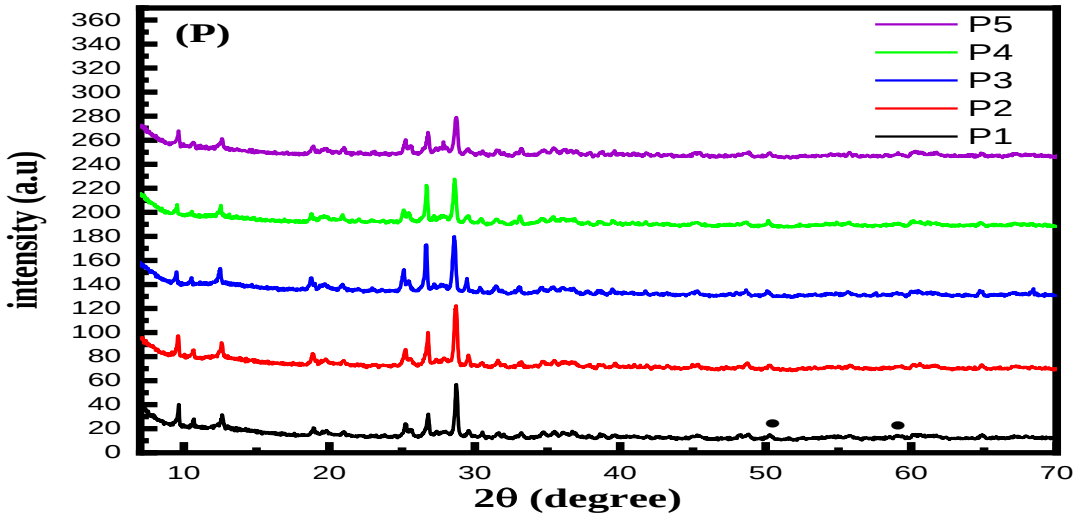

Fig. (13): The XRD for finished pottery products

7. CONCLUSION

In conclusion, the study provides a comprehensive assessment of the radiological characteristics of marl clay, Nile silt and pottery samples collected from handcrafted pottery sites in Hijaza, Qus, Qena, Upper Egypt. The analysis revealed that the natural radioactivity concentrations of key radionuclides, namely ^{238}U, ^{232}Th and ^{40}K, were significantly lower than the global average values reported by international organizations such as UNSCEAR. Furthermore, the calculated radiation hazard indices, including the radium equivalent, external and internal hazard indices and the excess lifetime cancer risk, all remained well below the safety limits recommended by global standards, indicating that the levels of radioactivity in the studied materials do not pose a significant radiological threat to human health.

These findings suggest that the materials used in handcrafted pottery production in the region do not contribute to harmful radiation exposure, thereby supporting the safe use of these raw materials in pottery manufacturing. The study assures that there is no significant radiological risk to workers or consumers exposed to these materials under normal conditions. Consequently, the marl clay, Nile silt and pottery samples from the studied area do not present a major radiological hazard, confirming their safety for traditional pottery production and use in the region.

REFERENCES

[1] Redmount, C. (2003). The Egyptian Modern Pottery Project: Pilot Phase Findings. In Egyptian Pottery, Proceedings of the 1990 Pottery Symposium at the University of California (pp. 153-322). ARF, Berkeley.

[2] Abulebda, M., Massaud, M., Mahran, I., & El-Mahdi, I. (2020). Some Aspects of Pottery's Significance in the Culture of the Ancient Egyptians. Journal of the Faculty of Tourism and Hotels-University of Sadat City, 4(1/1).

[3] Wodzinska, A. (2009). A Manual of Egyptian Pottery: Ptolemaic through Modern Period. A Manual of Egyptian Pottery, 1-350.

[4] Wodzinska, A. (2009). A Manual of Egyptian Pottery Volume 3: Second Intermediate Through Late Period (Vol. 3). ISD LLC.

[5] Abulebda, M., Massaud, M., Mahran, I., & El-Mahdi, I. (2020). Some Aspects of Pottery's Significance in the Culture of the Ancient Egyptians. Journal of the Faculty of Tourism and Hotels-University of Sadat City, 4(1/1).

[6] Guggenheim, S., Brady, J., Mogk, D., & Perkins, D. (1997). Introduction to the properties of clay minerals. Teaching Mineralogy (Eds: Brady, J. B, DW Mogk, D. Perkins). Mineralogical Society of America. Washington, DC, 371-388.

[7] Butzer, K. W. (1974). Modern Egyptian pottery clays and Predynastic buff ware. Journal of Near Eastern Studies, 33(4), 377-382.

[8] dos Santos Júnior, J. A., de Araújo, E. E. N., Fernández, Z. H., dos Santos Amaral, R., do Nascimento Santos, J. M., & Milán, M. O. (2021). Measurement of natural radioactivity and radium equivalent activity for pottery-making clay samples in Paraíba and Rio Grande do Norte–Brazil. Environmental Advances, 6, 100121.

[9] Abu Khadra, S. A., & Kamel, N. H. (2005). Natural Radioactivity in Ceramic Materials.

[10] El-Shershaby, A. (2003). Environmental isotopes and natural radioactivity assessment for clays, products derived from clay and radon exhalation rate of clays in Egypt. Environment Protection Engineering, 29(3-4), 25-40.

[11] Alharbi, W. R., & El-Taher, A. (2016). Elemental analysis and natural radioactivity levels of clay by γ-ray spectrometer and instrumental neutron activation analysis. Science and Technology of Nuclear Installations, 2016.

[12] Kranrod, C., Chanyotha, S., Pengvanich, P., Kritsananuwat, R., Hosoda, M., & Tokonami, S. (2020). A comparative study of the outdoor absorbed dose rate in the air by in-situ and soil-sampling-based measurement methods. Radiation Environment and Medicine, 9(2), 98-104.

[13] Qureshi, A. A., Ali, M., Waheed, A., Manzoor, S., Siddique, R. U. H., & Ahmed Khan, H. (2013). Assessment of radiological hazards of Lawrencepur sand, Pakistan using gamma spectrometry. Radiation protection dosimetry, 157(1), 73-84.

[14] El-Taher, A., Najam, L. A., Oraibi, A. H., & Isinkaye, M. O. (2017). Effect of Cement Factory Exhaust on Radiological Contents of Surrounding Soil Samples in Assuit Province, Egypt. Journal of Physical Science, 28(3), 137-150.

[15] ElTaher, A., Najam, L., Hussian, I., & Ali Omar, M. A. (2019). Evaluation of natural radionuclide content in Nile River sediments and excess lifetime cancer risk associated with gamma radiation. Iranian Journal of Medical Physics, 16(1), 27-33.

[16] Hilal, M. A., Attallah, M. F., Mohamed, G. Y., & Fayez-Hassan, M. (2014). Evaluation of radiation hazard potential of TENORM waste from oil and natural gas production. Journal of Environmental Radioactivity, 136, 121-126.

[17] Khater, A. E., Al-Mobark, L. H., Aly, A. A., & Al-Omran, A. M. (2013). Natural radionuclides in clay deposits: concentration and dose assessment. Radiation protection dosimetry, 156(3), 321-330.

[18] El-Khatib, A. A. Amany aboelkassem and H. Elz Responses of Urban Trees". International Journal of Current Rese Key words.

[19] Mahmoud, M. H., & El-Zohry, M. A. (2022). Radiological Impacts of Petroleum Exploration Activities in Ras Qattara Area, Northwestern Desert, Egypt. Arab Journal of Nuclear Sciences and Applications, 55(3), 46-54.

[20] dos Santos Júnior, J. A., de Araújo, E. E. N., Fernández, Z. H., dos Santos Amaral, R., do Nascimento Santos, J. M., & Milán, M. O. (2021). Measurement of natural radioactivity and radium equivalent activity for pottery-making clay samples in Paraíba and Rio Grande do Norte–Brazil. Environmental Advances, 6, 100121.

[21] El-Zohry, M. A. (2019). Radioactivity Concentrations in Dust and Soil of Enhanced Occurring Natural Radionuclides and Their Transfer Factors to Urban Trees in Phosphate Polluted Area. Arab Journal of Nuclear Sciences and Applications, 52(4), 93-99.

[22] Mahmoud, M. H. (2021). Study of Hazard Indices and Radiological Doses in Phosphate Samples from El-Mahamid Area, Upper-Egypt. Egyptian Journal of Physics, 49(1), 49-58.

[23] Shousha, H. A., Atta, M. R., Bakhit, A. A., Diab, H. M., El Hagg, A. A., &Dahy, S. (2019). Natural radioactivity assessment and the associated radiological hazards for beach sand, baltim area, Egypt. Al-Azhar Bulletin of Science, 30 (1-B), 37-47. 23.

[24] Arafa, W. (2004). Specific activity and hazards of granite samples collected from the Eastern Desert of Egypt. Journal of Environmental Radioactivity, 75(3), 315-327.

[25] Ediagbonya, T. F., Okungbowa, G. E., & Titilayo, O. (2020). Background Study of Natural Radioactivity in Soil. Journal of Chemical Society of Nigeria, 45(2).

[26] Taqi, A., & Namq, B. F. (2022). Radioactivity and Radionuclide Distribution in Jabel Bawr Oil Site of Kirkuk-Iraq. Arab Journal of Nuclear Sciences and Applications, 55(2), 113-124.

[27] Abdelmohsen, M. A., Farid, M. A. A., Uosif, M. A. M., & Alanany, S. (2018). ASSESSMENT OF NATURAL RADIOACTIVITY OF SOIL IN NEW ASSIUT CITY AND RADIOLOGICAL HAZARDS THAT EXPOSED POPULATION. ASSESSMENT, 47(2), 1-20.

[28] Badawy, W. M. (2009). Natural radioactivity of clay and sandy soils and radiation exposure doses in the Heet and Inshass regions of Egypt. Moscow University Soil Science Bulletin, 64, 105-107.

[29] Śleziak, M., Petryka, L., & Zych, M. (2010). Natural radioactivity of soil and sediment samples collected from postindustrial areas. Polish J. of Envir. Studies, 19(5), 1095-99.

[30] Korany, K., & Yousef, H. (2019). Assessment of Radiological Hazard Indices in Abu Rusheid area, Southeastern Desert, Egypt, Using Gamma-Ray Spectroscopy. Arab Journal of Nuclear Sciences and Applications, 52(2), 132-141.

[31] Ibraheem, A. A., El-Taher, A., & Alruwaili, M. H. (2018). Assessment of natural radioactivity levels and radiation hazard indices for soil samples from Abha, Saudi Arabia. Results in Physics, 11, 325-330.

[32] Amana, M. S. (2017). Radiation hazard index of commonly imported ceramic used for building materials in Iraq. Aust. J. Basic. Appl. Sci, 11(10), 94-102.

[33] Natural Radioactivity Measurement and Assessment of Radiological Hazards in Some Building Materials Used in Bangladesh.

[34] Joel, E. S., De, D. K., Omeje, M., Adewoyin, O., Olawole, O. C., Akinwumi, A., ... & Adeyemi, G. A. (2020). Assessment of background radionuclides and gamma dose rate distribution in Urban-setting and its radiological significance. Scientific African, 8, e00377.

[35] Mubarak, F., Fayez-Hassan, M., Mansour, N. A., Salah Ahmed, T., & Ali, A. (2017). Radiological investigation of high background radiation areas. Scientific reports, 7(1), 15223.

[36] Abojassim, A. A., & Rasheed, L. H. (2019). Mapping of terrestrial gamma radiation in soil samples at Baghdad governorate (Karakh side), using GIS technology. Nature Environment and Pollution Technology, 18(4), 1095-1106.

[37] E. Ekpe, E., Ben, U. C., Ekwok, S. E., Ebong, E. D., Akpan, A. E., Eldosouky, A. M., ... & Gómez-Ortiz, D. (2022). Assessment of Natural Radionuclide Distribution Pattern and Radiological Risk from Rocks in Precambrian Oban Massif, Southeastern Nigeria. Minerals, 12(3), 312.

[38] Murugesan, S., & Ravichandran, S. (2023). Radioactive heat production rate and excess lifetime cancer risk of sand from two major rivers in India–A comparative study. International Journal of Radiation Research, 21(1), 117-124.

[39] Avwiri, G. O., Ononugbo, C. P., & Nwokeoji, I. E. (2014). Radiation Hazard Indices and Excess Lifetime Cancer Risk in Soil, Sediment and Water around mini-okoro/Oginigba Creek, Port Harcourt, Rivers State, Nigeria. Comprehensive Journal of Environment and Earth Sciences, 3(1), 38-50.

[40] Alharshan, G. A., Kamar, M. S., Lasheen, E. S. R., Ene, A., Uosif, M. A., Awad, H. A., & Zakaly, H. M. (2022). Distribution of Radionuclides and Radiological Health Assessment in Seih-Sidri Area, Southwestern Sinai. International Journal of Environmental Research and Public Health, 19(17), 10717.

[41] UNSCEAR (2000) Sources and effects of ionizing radiation. In United Nations Scientific Committee on the effect of atomic radiation, U.N., NY (ed). New York.

[42] UNSCEAR (2008). United Nations, and Scientific Committee on the Effects of Atomic Radiation. Report of the United Nations Scientific Committee on the effects of atomic radiation: Fifty-sixth Session. United Nations Publications (10-18 July 2008) (No. 46).

[43] ICRP, I. (1991). 1990 recommendations of the International Commission on Radiological Protection. Annals of the ICRP, 21, 201.